2. Heppner GH. Tumor heterogeneity. Cancer Res 1984;44:2259–2265.
3. Hanahan D, Weinberg RA. The hallmarks of cancer. Cell 2000; 100:57–70.
4. Jordan CT, Guzman ML, Noble M. Cancer stem cells. N Engl J Med 2006;355:1253–1261.
5. Clarke MF, Dick JE, Dirks PB, et al. Cancer stem cells—perspectives on current status and future directions: AACR Workshop on cancer stem cells. Cancer Res 2006;66:9339–9344.
6. Potter VR. Phenotypic diversity in experimental hepatomas: the concept of partially blocked ontogeny. The 10th Walter Hubert Lecture. Br J Cancer 1978;38:1–23.
7. Sell S. Cellular origin of cancer: dedifferentiation or stem cell maturation arrest? Environ Health Perspect 1993;101(Suppl 5): 15–26.
8. Wicha MS, Liu S, Dontu G. Cancer stem cells: an old idea—a paradigm shift. Cancer Res 2006;66:1883–1890.
9. Al Hajj M, Wicha MS, Benito-Hernandez A, et al. Prospective identification of tumorigenic breast cancer cells. Proc Natl Acad Sci U S A 2003;100:3983–3988.
10. Singh SK, Hawkins C, Clarke ID, et al. Identification of human brain tumour initiating cells. Nature 2004;432:396–401.
11. Bonnet D, Dick JE. Human acute myeloid leukemia is organized as a hierarchy that originates from a primitive hematopoietic cell. Nat Med 1997;3:730–737.
12. Ricci-Vitiani L, Lombardi DG, Pilozzi E, et al. Identification and expansion of human colon-cancer-initiating cells. Nature 2007; 445:111–115.
13. O'Brien CA, Pollett A, Gallinger S, et al. A human colon cancer cell capable of initiating tumour growth in immunodeficient mice. Nature 2007;445:106–110.
14. Dean M, Fojo T, Bates S. Tumour stem cells and drug resistance. Nat Rev Cancer 2005;5:275–284.
15. Rich JN. Cancer stem cells in radiation resistance. Cancer Res 2007;67:8980–8984.
16. Parkin DM, Bray F, Ferlay J, et al. Global cancer statistics, 2002. CA Cancer J Clin 2005;55:74–108.
17. Sell S, Pierce GB. Maturation arrest of stem cell differentiation is a common pathway for the cellular origin of teratocarcinomas and epithelial cancers. Lab Invest 1994;70:6–22.
18. Thorgeirsson SS, Grisham JW. Hepatic stem cells. Semin Liver Dis 2003;23:301.
19. Thorgeirsson SS, Grisham JW. Molecular pathogenesis of human hepatocellular carcinoma. Nat Genet 2002;31:339–346.
20. Lee JS, Heo J, Libbrecht L, et al. A novel prognostic subtype of human hepatocellular carcinoma derived from hepatic progenitor cells. Nat Med 2006;12:410–416.
21. Sigal SH, Brill S, Fiorino AS, et al. The liver as a stem cell and lineage system. Am J Physiol 1992;263:G139–G148.
22. Schmelzer E, Wauthier E, Reid LM. The phenotypes of pluripotent human hepatic progenitors. Stem Cells 2006;24:1852–1858.
23. Schmelzer E, Zhang L, Bruce A, et al. Human hepatic stem cells from fetal and postnatal donors. J Exp Med 2007;204:1973–1987.
24. Dan YY, Riehle KJ, Lazaro C, et al. Isolation of multipotent progenitor cells from human fetal liver capable of differentiating into liver and mesenchymal lineages. Proc Natl Acad Sci U S A 2006;103:9912–9917.
25. Zaret KS. Regulatory phases of early liver development: paradigms of organogenesis. Nat Rev Genet 2002;3:499–512.
26. Shafritz DA, Oertel M, Menthena A, et al. Liver stem cells and prospects for liver reconstitution by transplanted cells. Hepatology 2006;43:S89–S98.
27. Yamashita T, Forgues M, Wang W, et al. EpCAM and alpha-fetoprotein expression defines novel prognostic subtypes of hepatocellular carcinoma. Cancer Res 2008;68:1451–1461.
28. Reya T, Clevers H. Wnt signalling in stem cells and cancer. Nature 2005;434:843–850.
29. Yamashita T, Budhu A, Forgues M, et al. Activation of hepatic stem cell marker EpCAM by Wnt-β-catenin signaling in hepatocellular carcinoma. Cancer Res 2007;67:10831–10839.
30. Budhu A, Forgues M, Ye QH, et al. Prediction of venous metastases, recurrence and prognosis in hepatocellular carcinoma based on a unique immune response signature of the liver microenvironment. Cancer Cell 2006;10:99–111.
31. Ye QH, Qin LX, Forgues M, et al. Predicting hepatitis B virus-positive metastatic hepatocellular carcinomas using gene expression profiling and supervised machine learning. Nat Med 2003;9:416–423.
32. Wu CG, Forgues M, Siddique S, et al. SAGE transcript profiles of normal primary human hepatocytes expressing oncogenic hepatitis B virus X protein. FASEB J 2002;16:1665–1667.
33. Kubota H, Reid LM. Clonogenic hepatoblasts, common precursors for hepatocytic and biliary lineages, are lacking classical major histocompatibility complex class I antigen. Proc Natl Acad Sci U S A 2000;97:12132–12137.
34. Yoshikawa H, Matsubara K, Zhou X, et al. WNT10B functional dualism: beta-catenin/Tcf-dependent growth promotion or independent suppression with deregulated expression in cancer. Mol Biol Cell 2007;18:4292–4303.
35. Yang ZF, Ho DW, Ng MN, et al. Significance of CD90(+) cancer stem cells in human liver cancer. Cancer Cell 2008;13:153–166.
36. Dontu G, Abdallah WM, Foley JM, et al. In vitro propagation and transcriptional profiling of human mammary stem/progenitor cells. Genes Dev 2003;17:1253–1270.
37. Fang D, Nguyen TK, Leishear K, et al. A tumorigenic subpopulation with stem cell properties in melanomas. Cancer Res 2005; 65:9328–9337.
38. Sato N, Meijer L, Skaltsounis L, et al. Maintenance of pluripotency in human and mouse embryonic stem cells through activation of Wnt signaling by a pharmacological GSK-3-specific inhibitor. Nat Med 2004;10:55–63.
39. Balzar M, Winter MJ, de Boer CJ, et al. The biology of the 17-1A antigen (Ep-CAM). J Mol Med 1999;77:699–712.
40. Trzpis M, McLaughlin PM, de Leij LM, et al. Epithelial cell adhesion molecule: more than a carcinoma marker and adhesion molecule. Am J Pathol 2007;171:386–395.
41. Dalerba P, Dylla SJ, Park IK, et al. Phenotypic characterization of human colorectal cancer stem cells. Proc Natl Acad Sci U S A 2007;104:10158–10163.
42. Ma S, Chan KW, Hu L, et al. Identification and characterization of tumorigenic liver cancer stem/progenitor cells. Gastroenterology 2007;132:2542–2556.
43. Yin AH, Miraglia S, Zanjani ED, et al. AC133, a novel marker for human hematopoietic stem and progenitor cells. Blood 1997;90: 5002–5012.
44. Fargeas CA, Corbeil D, Huttner WB. AC133 antigen, CD133, prominin-1, prominin-2, etc.: prominin family gene products in need of a rational nomenclature. Stem Cells 2003;21:506–508.
45. Shmelkov SV, Butler JM, Hooper AT, et al. CD133 expression is not restricted to stem cells, and both CD133+ and CD133- metastatic colon cancer cells initiate tumors. J Clin Invest 2008; 118:2111–2120.
46. Hill RP, Perris R. "Destemming" cancer stem cells. J Natl Cancer Inst 2007;99:1435–1440.
47. Piccirillo SG, Reynolds BA, Zanetti N, et al. Bone morphogenetic proteins inhibit the tumorigenic potential of human brain tumour-initiating cells. Nature 2006;444:761–765.
48. Munz M, Kieu C, Mack B, et al. The carcinoma-associated antigen EpCAM upregulates c-myc and induces cell proliferation. Oncogene 2004;23:5748–5758.

49. Takahashi K, Tanabe K, Ohnuki M, et al. Induction of pluripotent stem cells from adult human fibroblasts by defined factors. Cell 2007;131:861–872.
50. Chaudry MA, Sales K, Ruf P, et al. EpCAM an immunotherapeutic target for gastrointestinal malignancy: current experience and future challenges. Br J Cancer 2007;96:1013–1019.
51. Nagrath S, Sequist LV, Maheswaran S, et al. Isolation of rare circulating tumour cells in cancer patients by microchip technology. Nature 2007;450:1235–1241.

Received March 9, 2008. Accepted December 1, 2008.

Reprint requests

Address requests for reprints to: Xin Wei Wang, PhD, Liver Carcinogenesis Section, Laboratory of Human Carcinogenesis, Center for Cancer Research, National Cancer Institute, 37 Convent Drive, Building 37, Room 3044A, MSC 4258, Bethesda, Maryland 20892-4258. e-mail: xw3u@nih.gov; fax: (301) 496-0497.

Acknowledgments

Microarray data are available publicly at http://www.ncbi.nlm.nih.gov/geo/ (accession number: GSE5975).

The authors thank Drs Curtis Harris and Sharon Pine for critical readings of the manuscript; Ms Barbara Taylor and Dr Susan Garfield for technical assistance; Drs Ali Brivanlou (Rockefeller University), Steve Strom (University of Pittsburgh), and Bert Vogelstein (Johns Hopkins University) for generously providing their research materials.

Conflicts of Interest

The authors disclose no conflicts.

Funding

The authors disclose the following: This work was supported in part by the Intramural Research Program of the Center for Cancer Research, the US National Cancer Institute. Dr Yang, Dr HY Wang, Dr Jia, Dr Ye, Dr Qin, and Dr Tang were supported by research grants from the China National Natural Science Foundation for Distinguished Young Scholars (30325041) and the China National "863" R&D High-Tech Key Project (2002BA711A02-4). Dr Reid was supported by a sponsored research grant from Vesta Therapeutics (Research Triangle Park, NC), National Institutes of Health grants (RO1 AA014243 and RO1 IP30-DK065933), and a US Department of Energy grant (DE-FG02-02ER-63477). Sponsors had no role in the study design, data collection, analysis, and interpretation. Dr Yamashita, Dr Ji, Dr Budhu, Dr Forgues, Dr Yang, Dr Wang, Dr Jia, Dr Ye, Dr Wauthier, Dr Minato, Dr Honda, Dr Kaneko, and Dr Wang disclose no conflicts.

Supplementary Materials and Methods

FACS and MACS Analyses

Cultured cells were trypsinized, washed, and resuspended in Hank's balanced salt solutions (Lonza, Basel, Switzerland) supplemented with 1% HEPES and 2% fetal bovine serum. Cells then were incubated with FITC-conjugated anti-EpCAM monoclonal antibody Clone Ber-EP4 (DAKO, Carpinteria, CA) on ice for 30 minutes, and $EpCAM^+$ and $EpCAM^-$ cells were isolated by a BD FACSAria cell sorting system (BD Biosciences). For magnetic separation, cells were labeled 24 hours after enzymatic dissociation with primary EpCAM antibody (mouse IgG1; Dako), subsequently magnetically labeled with rat anti-mouse IgG1 Microbeads, and separated on a MACS LS column (Miltenyi Biotec, Inc, Auburn, CA). All the procedures were performed according to the manufacturer's instructions. The purity of sorted cells was evaluated by FACS. Fixed cells also were analyzed by FACS using a FACSCalibur (BD Biosciences). Anti-EpCAM antibody VU-1D9, anti-CD133/2 clone 293C3 (Miltenyi Biotec Inc), and anti-CD90 clone 5E10 (StemCell Technologies Inc, Vancouver, British Columbia, Canada) were used to detect $EpCAM^+$, $CD133^+$, or $CD90^+$ cells. Intracellular AFP levels were examined by a BD Cytofix/Cytoperm Fixation/Permeabilization Kit (San Jose, CA) and anti-AFP rabbit polyclonal antibody (DAKO).

Quantitative Reverse Transcription–Polymerase Chain Reaction and IHC Analyses

Total RNA was extracted using TRIzol (Invitrogen) according to the manufacturer's instructions. The expression of selected genes was determined in triplicate using the Applied Biosystems 7500 Sequence Detection System (Applied Biosystems, Foster City, CA) as previously described.[1] Genes expressed in embryonic stem cells were determined in quadruplicate using TaqMan Human Stem Cell Pluripotency Array (Applied Biosystems). IHC analyses with specific antibodies were performed essentially as previously described.[1] Confocal fluorescence microscopic analysis was performed essentially as previously described.[2]

References

1. Yamashita T, Forgues M, Wang W, et al. EpCAM and alpha-fetoprotein expression defines novel prognostic subtypes of hepatocellular carcinoma. Cancer Res 2008;68:1451–1461.
2. Wang W, Budhu A, Forgues M, et al. Temporal and spatial control of nucleophosmin by the Ran-Crm1 complex in centrosome duplication. Nat Cell Biol 2005;7:823–830.

Supplemetary Table 1. Clinicopathologic Characteristics of HpSC-HCC and MH-HCC Cases Used for Oligonucleotide Microarray Analyses

Parameters	HpSC-HCC (n = 60)	MH-HCC (n = 96)	*P* value[a]
Mean age, *y* (SD)	46.0 ± 10.7	52.9 ± 10.5	.0004
Sex: male/female	50/10	87/9	.18
Cirrhosis: yes/no/no data	56/4	88/7/1	.72
Median AFP level, *ng/mL* (25%–75%)	1706 (865–5915)	11.8 (4.0–48.6)	<.0001
Histologic grade[b]			
I–II	14	41	
II–III	44	48	
III–IV	2	5	
No data	0	2	.031
Mean tumor size, *cm* (SD)	5.1 ± 3.0	4.4 ± 3.0	.088
Multinodular: yes/no	16/44	15/81	.09
Portal vein invasion, yes/no[c]	11/49	9/87	.10
TNM classification			
I	24	46	
II	22	42	
III	14	8	.03
Virus status: HBV/HBV + HCV/unknown	56/4/0	95/0/1	.43

[a]Mann–Whitney *U* test or χ^2 test.
[b]Edmondson–Steiner.
[c]Macroscopic portal vein invasion.

Supplementary Table 2. Clinicopathologic Characteristics of HpSC-HCC and MH-HCC Cases Used for IHC

Parameters	HpSC-HCC (n = 24)	MH-HCC (n = 55)	*P* value[a]
Mean age, *y* (SD)	46.4 ± 9.4	58.4 ± 11.9	< .0001
Sex: male/female	20/4	48/7	.64
Cirrhosis: yes/no	23/1	46/9	.14
Median AFP level, *ng/mL* (25%–75%)	1620 (887–3166)	12 (9.3–219)	< .0001
Histologic grade[b]			
I–II	12	32	
II–III	8	21	
III–IV	4	2	.13
Mean tumor size, *cm* (SD)	7.1 ± 3.6	5.2 ± 3.6	.014
Multinodular: yes/no	4/20	16/39	.24
Portal vein invasion: yes/no[c]	12/12	12/43	.012
TNM classification			
I	4	19	
II	8	20	
III	12	16	.14
Virus status: HBV/HCV/unknown	21/2/1	32/21/2	.026

[a]Mann–Whitney *U* test or χ^2 test.
[b]Edmondson–Steiner.
[c]Macroscopic portal vein invasion.

Supplementary Table 3. Top 10 List of Canonical Pathways Activated in HpSC-HCC From Ingenuity Pathway Analysis

Pathways	Genes included in cluster A
Axonal guidance signaling	
Up	ROBO2, ARPC5L (includes EG:81873), SEMA4G, PDGFRB, PLCB1, PRKCD, FGFR3, FZD5, MERTK, DDR1, LINGO1, SEMA3C
Down	PIK3C3, IGF1, PIK3C2G, MAP2K2, ARHGEF15
Transforming growth factor-β signaling	
Up	PDGFRB, FGFR3, MERTK, UBD, DDR1, SMAD5
Down	MAP2K2, HNF4A
Integrin signaling	
Up	ARPC5L (includes EG:81873), PDGFRB, FGFR3, GRB7, MERTK, ITGB5, DDR1, DDEF1
Down	PIK3C3, MYLK, PIK3C2G, MAP2K2
Apoptosis signaling	
Up	PDGFRB, BAK1, CYCS, FGFR3, MERTK, DDR1
Down	MAP3K5, MAP2K2
G2/M DNA damage checkpoint regulation	
Up	YWHAZ, CCNB2, UBD, WEE1
Down	CDKN2A, GADD45A
ERK/MAPK signaling	
Up	ELF3, PDGFRB, YWHAZ, PRKCD, FGFR3, MERTK, DDR1
Down	PIK3C3, DUSP1, PIK3C2G, ESR1, MAP2K2
Wnt/β-catenin signaling	
Up	DKK1, SOX9, FZD5, UBD, TCF7L2, CSNK1E
Down	CDKN2A, RARG
PI3K/AKT signaling	
Up	PDGFRB, YWHAZ, FGFR3, MERTK, DDR1
Down	MAP3K5, MAP2K2, GYS2
Amyloid processing	
Up	BACE2, CSNK1E, MAPK13
Down	
Leukocyte extravasation signaling	
Up	PRKCD, CLDN4, CLDN1, MMP11, MAPK13
Down	PIK3C3, CLDN2, PIK3C2G, MAP2K2

NOTE. The top 10 pathways were selected based on the significance for the enrichment of the genes with a particular canonical signaling pathway determined by the one-sided Fisher exact test ($P < .01$).

Supplementary Table 4. Top 10 List of Canonical Pathways Activated in MH-HCC From Ingenuity Pathway Analysis

Pathways	Genes included in cluster B
Lipopolysaccharide/interleukin-1–mediated inhibition of RXR function	
Up	SULT1C2, ACSL4, ACSL3, FABP5, GSTP1
Down	NR1I2, NR1I3, CYP7A1, ALDH1L1, ABCB1, SLC10A1, SLC27A2, CD14, GSTM1, ALDH6A1, GSTM4, ACSL5, CES2 (includes EG:8824), FMO3, SULT2A1 (includes EG:6822), GSTA1, CYP2C8, LC27A5, CYP3A7, ABCG5, ALDH8A1, APOC4 (includes EG:346), CYP3A4, ACSL1, ABCB11, FMO4, MAOA
Xenobiotic metabolism signaling	
Up	SULT1C2, PRKCD, GSTP1, MAPK13
Down	NR1I2, NR1I3, ALDH1L1, ABCB1, UGT2B15, MAP2K2, UGT2B7, PPARGC1A, GSTM1, PIK3C3, ALDH6A1, GSTM4, CES2 (includes EG:8824), MAP3K5, FMO3, PIK3C2G, SULT2A1 (includesEG:6822), CYP1A2, GSTA1, CYP2C8, CYP3A7, NQO2, ALDH8A1, CYP3A4, CES1 (includes EG:1066), FMO4, MAOA
Hepatic cholestasis	
Up	ADCY3, PRKCD
Down	CD14, ABCG5, NR1I2, CYP7A1, CYP7B, CYP8B1, ABCB1, ESR1, SLC10A1, ABCB11, ABCB4, HNF4A
Aryl hydrocarbon receptor signaling	
Up	GSTP1
Down	CDKN2A, NQO2, GSTM1, ALDH8A1, ALDH6A1, ALDH1L1, GSTM4, ESR1, CYP1A2, GSTA1, RARG
NRF2-mediated oxidative stress response	
Up	DNAJA4, PRKCD, GSTP1
Down	NQO2, GSTM1, AOX1, PIK3C3, GSTM4, MAP3K5, SOD1, PIK3C2G, MAP2K2, FKBP5, GSTA1
Complement system	
Up	
Down	C8A, C1R, MASP1, C6, C8B, MASP2
Coagulation system	
Up	
Down	SERPINC1, KLKB1, F9, KNG1 (includes EG:3827), F11
Acute-phase response signaling	
Up	MAPK13
Down	APCS, RBP5, C1R, MAP3K5, HRG, MAP2K2, KLKB1, SAA4
p53 signaling	
Up	THBS1
Down	CDKN2A, PIK3C3, SNAI2, GADD45A, PIK3C2G, GADD45B
LXR/RXR activation	
Up	HMGCR
Down	CD14, ABCG5, APOA5, CYP7A1, APOC4 (includes EG:346)

LXR/RXR, liver X receptor/retinoid X receptor; NRF2, NF-E2-related factor 2.
NOTE. The top 10 pathways were selected based on the significance for the enrichment of the genes with a particular canonical signaling pathway determined by the one-sided Fisher exact test ($P < .01$).

ELSEVIER

Journal of Hepatology 50 (2009) 100–110

Journal of Hepatology

www.elsevier.com/locate/jhep

Activation of lipogenic pathway correlates with cell proliferation and poor prognosis in hepatocellular carcinoma☆

Taro Yamashita[1], Masao Honda[1,2], Hajime Takatori[1], Ryuhei Nishino[1], Hiroshi Minato[3], Hiroyuki Takamura[4], Tetsuo Ohta[4], Shuichi Kaneko[1,*]

[1]*Department of Gastroenterology, Kanazawa University Graduate School of Medical Science, 13-1 Takara-Machi, Kanazawa 920-8641, Japan*
[2]*Department of Advanced Medical Technology, Kanazawa University School of Health Sciences, 13-1 Takara-Machi, Kanazawa 920-8641, Japan*
[3]*Pathology Section, Kanazawa University Hospital, 13-1 Takara-Machi, Kanazawa 920-8641, Japan*
[4]*Department of Gastroenterologic Surgery, Kanazawa University Graduate School of Medical Science, 13-1 Takara-Machi, Kanazawa 920-8641, Japan*

***Background/Aims*: Metabolic dysregulation is one of the risk factors for the development of hepatocellular carcinoma (HCC). We investigated the activated metabolic pathway in HCC to identify its role in HCC growth and mortality.**

***Methods*: Gene expression profiles of HCC tissues and non-cancerous liver tissues were obtained by serial analysis of gene expression. Pathway analysis was performed to characterize the metabolic pathway activated in HCC. Suppression of the activated pathway by RNA interference was used to evaluate its role in HCC *in vitro*. Relation of the pathway activation and prognosis was statistically examined.**

***Results*: A total of 289 transcripts were up- or down-regulated in HCC compared with non-cancerous liver ($P < 0.005$). Pathway analysis revealed that the lipogenic pathway regulated by sterol regulatory element binding factor 1 (*SREBF1*) was activated in HCC, which was validated by real-time RT-PCR. Suppression of *SREBF1* induced growth arrest and apoptosis whereas overexpression of *SREBF1* enhanced cell proliferation in human HCC cell lines. *SREBF1* protein expression was evaluated in 54 HCC samples by immunohistochemistry, and Kaplan–Meier survival analysis indicated that *SREBF1*-high HCC correlated with high mortality.**

***Conclusions*: The lipogenic pathway is activated in a subset of HCC and contributes to cell proliferation and prognosis.**
© 2008 European Association for the Study of the Liver. Published by Elsevier B.V. All rights reserved.

***Keywords*: Hepatocellular carcinoma; Serial analysis of gene expression; Lipogenesis; Gene expression profiling; Sterol regvulatory element binding factor 1**

Received 26 May 2008; received in revised form 1 July 2008; accepted 23 July 2008; available online 12 October 2008
Associate Editor: J.M. Llovet

☆ The authors who have taken part in the research of this paper declared that they do not have a relationship with the manufacturers of the materials involved either in the past or present and they did not receive funding from the manufacturers to carry out their research.

* Corresponding author. Tel.: +81 76 265 2231; fax: +81 76 234 4250.
E-mail address: skaneko@m-kanazawa.jp (S. Kaneko).

Abbreviations: HCC, hepatocellular carcinoma; *SREBF1*, sterol regulatory element binding factor 1; HBV, hepatitis B virus; HCV, hepatitis C virus; SAGE, serial analysis of gene expression; RT-PCR, reverse transcription-polymerase chain reaction; IHC, immunohistochemistry; FADS1, fatty acid desaturase 1; SCD, stearoyl CoA desaturase; FASN, fatty acid synthase; si-RNA, short interfering-RNA; CLD, chronic liver disease; PCNA, proliferating cell nuclear antigen; IGF, insulin-like growth factor.

1. Introduction

Hepatocellular carcinoma (HCC) is one of the most frequently occurring malignancies in the world [1]. The major risk factors associated with HCC include chronic infection with hepatitis B virus (HBV) and hepatitis C virus (HCV), alcohol abuse, and exposure to aflatoxin B1 [2]. HCC usually develops from liver cirrhosis, which involves continuous inflammation and hepatocyte regeneration, suggesting that reactive oxygen species and DNA damage are involved in the process of hepatocarcinogenesis [3].

The development of gene expression profiling technologies including DNA microarrays and serial analysis

0168-8278/$34.00 © 2008 European Association for the Study of the Liver. Published by Elsevier B.V. All rights reserved.
doi:10.1016/j.jhep.2008.07.036

of gene expression (SAGE) have enhanced our ability to identify inventory transcripts and global genetic alterations in HCC [4–10]. In general, these methods have demonstrated that transcripts associated with cell growth are up-regulated, whereas those related to inhibition of cell growth are down-regulated, in HCC [11]. It is difficult, however, to decipher molecular pathways activated during hepatocarcinogenesis.

Epidemiological studies suggest that metabolic dysregulation in the liver increases the risk of HCC development. For example, diabetes is associated with a 2-fold increase in the risk of HCC [12]. Obesity and hepatic steatosis also increase the risk of HCC [13–15]. Furthermore, recent studies indicate that HCV infection provokes hepatic steatosis, which may be a vulnerable factor for liver inflammation and HCC development [16,17]. Thus, dysregulation of a metabolic pathway may play a crucial role to promote HCC growth, but the molecular mechanism is still obscure. In this study, we have utilized SAGE [18,19], which enables us to monitor the differential expression of all genes, to determine the global changes in gene expression that occur during hepatocarcinogenesis.

2. Materials and methods

2.1. Tissue samples

All HCC tissues, adjacent non-cancerous liver tissues, and normal liver tissues were obtained from 69 patients who underwent hepatectomy from 1997 to 2005 in Kanazawa University Hospital. Normal liver tissue samples were obtained from patients undergoing surgical resection of the liver for treatment of metastatic colon cancer. HCC and surrounding non-cancerous liver samples were obtained from patients undergoing surgical resection of the liver for the treatment of HCC. The samples used for SAGE, real-time reverse-transcription (RT)-PCR analysis, and immunohistochemistry (IHC) are listed in Supplemental Table 1. All samples used for SAGE and real-time RT-PCR analysis were snap-frozen in liquid nitrogen. Four normal liver tissues and 20 HCCs and their corresponding non-cancerous liver tissues were used for real-time RT-PCR analysis; seven of these HCC samples, along with 47 additional HCC samples, were formalin-fixed paraffin-embedded and used for IHC. HCC and adjacent non-cancerous liver were histologically characterized as described [20].

All strategies used for gene expression analysis as well as tissue acquisition processes were approved by the Ethics Committee and the Institutional Review Board of Kanazawa University Hospital. All procedures and risks were explained verbally, and each patient provided written informed consent.

2.2. SAGE

Total RNA was purified from each homogenized tissue sample using a ToTally RNA extraction kit (Ambion, Inc., Austin, TX), and polyadenylated RNA was isolated using a MicroPoly (A) Pure kit (Ambion). A total of 2.5 μg mRNA per sample was analyzed by SAGE [18]. SAGE libraries were randomly sequenced at the Genomic Research Center (Shimadzu-Biotechnology, Kyoto, Japan), and the sequence files were analyzed with SAGE 2000 software. The size of each SAGE library was normalized to 300,000 transcripts per library, and the abundance of transcripts was compared by SAGE 2000 software. Monte Carlo simulation was used to select genes with significant differences in expression between two libraries without multiple hypothesis testing correction ($P < 0.005$) [21]. Each SAGE tag was annotated using a gene-mapping web site (http://www.ncbi.nlm.nih.gov/SAGE/index.cgi).

2.3. Analysis of signaling networks

Ingenuity Pathways Analysis software (Ingenuity® Systems, www.ingenuity.com) was used to investigate the molecular pathways activated in an HCC SAGE library compared with an adjacent non-cancerous liver SAGE library. All reliable transcripts statistically up-regulated in HCC were investigated and annotated with biological processes, protein-protein interactions, and gene regulatory networks, using a reference-based data file with statistical significance. All identified pathways were screened individually. MetaCore™ software (GeneGo Inc., St. Joseph, MI) was used to evaluate candidate transcription factors responsible for up-regulation of transcripts in HCC.

2.4. RT-PCR

A 1-μg aliquot of each total RNA was reverse-transcribed using SuperScript II reverse-transcriptase (Invitrogen, Carlsbad, CA). Real-time RT-PCR analysis was performed using ABI PRISM 7900 Sequence Detection System (Applied Biosystems, Foster City, CA). Using the standard curve method, quantitative **PCR** was performed in triplicate for each sample-primer set. Each sample was normalized relative to β-actin. The assay IDs used were Hs00231674_m1 for sterol regulatory element binding factor 1 (*SREBF1*); Hs00203685_m1 for fatty acid desaturase 1 (*FADS1*) ;Hs00748952_s1 for stearoyl CoA desaturase (*SCD*); Hs001 88012_m1 for fatty acid synthase (*FASN*); and Hs99999_m1 for β-actin. *SREBF1a* and *SREBF1c* mRNA levels were assayed by semi-quantitative RT-PCR [22].

2.5. RNA Interference targeting SREBF1

Si-RNAs targeting *SREBF1* were constructed using a *Silencer*™ SiRNA Construction kit (Ambion) according to the manufacturer's protocol. We constructed two different si-RNAs, targeting different sites of *SREBF1* (*SREBF1*-1; CAGTGGCACTGACTCTTCC, *SREBF1*-2; TCTACGACCAGTGGGACTG). Control si-RNA duplexes targeting scramble sequences were also synthesized (Dharmacon Research, Inc., Lafayette, CO). Lipofectamine 2000™ reagent (Invitrogen) was used for transfection according to the manufacturer's instructions.

2.6. Cell proliferation assay

Cell proliferation assays were performed using a Cell Titer96 Aqueous kit (Promega, Madison, WI). Results are expressed as the mean optical density (OD) of each five-well set. All experiments were repeated at least twice.

2.7. Soft agar assay

To each well of a six-well plate, containing a base layer of 0.72% agar in growth medium, was added 1×10^4 cells, suspended in 2 ml of 0.36% agar with growth medium (DMEM supplemented with 10% FBS), and the plates were incubated at 37 °C in a 5% CO_2 incubator for 2 weeks. The numbers of colonies in each well were counted as previously described [23].

2.8. TUNEL assay

A DeadEnd™ Colorimetric TUNEL System (Promega) was used to measure nuclear DNA fragmentation as described previously [24].

2.9. Annexin V staining

To evaluate apoptotic cell death, Annexin V binding to cell membranes was evaluated using Annexin V-FITC antibodies and FACSCalibur flow cytometer (BD Biosciences, Franklin Lakes, NJ), as described by the manufacturer.

2.10. Focus assay

HuH7 cells and Hep3B cells were transiently transfected with pCMV7 or pCMV7-*SREBF1c* vectors (kindly provided by Dr. Hitoshi Shimano) using Lipofectamine 2000™ reagent (Invitrogen), as described by the manufacturer. A total of 2×10^3 cells were seeded on six-well plates 48 h after transfection, and cultured in usual media with 400 ng/ml of Geneticin for 9 days. The foci were fixed with ice-cold 100% methanol and stained with 0.5% crystal violet solution. All experiments were performed in triplicates.

2.11. Western blotting

Whole cell lysates were prepared using RIPA lysis buffer. Antibodies used were rabbit polyclonal antibodies to phospho-GSK-3β (ser9) (Cell Signaling Technology Inc., Danvers, MA), rabbit anti-sterol regulatory element binding protein-1 (encoded by *SREBF1*) polyclonal antibody H-160 (Santa Cruz Biotechnology, Inc., Santa Cruz, CA), and β-actin (Sigma-Aldrich Japan K.K., Tokyo, Japan). Immune complexes were visualized by enhanced chemiluminescence (Amersham Biosciences Corp., Piscataway, NJ) as described in the manufacturer's protocol.

2.12. Immunohistochemistry

Rabbit anti-*SREBF1* polyclonal antibody H-160 (Santa Cruz Biotechnology, Inc.) and mouse anti-proliferating cell nuclear antigen (PCNA) monoclonal antibody PC10 (Calbiochem, San Diego, CA) were used to evaluate the immunoreactivity of HCC samples, using a DAKO EnVision+™ Kit, as described by the manufacturer. The signal intensity of *SREBF1* was scored as negative, low, or high determined by the representative staining of the normal liver tissue and cirrhotic liver tissue (Supplemental Fig. 1). HCC was referred as *SREBF1*-high if *SREBF1* expression in the tumor was higher than that in the cirrhotic liver tissue. PCNA index was evaluated as previously described [25].

2.13. Statistical analysis

Kruskal–Wallis test was used to compare the differentially expressed genes, as shown by real-time PCR, among normal liver, CLD, and HCC tissues. Mann–Whitney U test was also used to evaluate the statistical significance of differences of gene expression between CLD and HCC tissues. Spearman's correlation coefficient was used to assess correlations between the expression levels of *SREBF1*, *FADS1*, *SCD*, and *FASN*. Univariate Cox proportional hazards regression analysis was used to evaluate the association of gene expression and clinicopathologic parameters with patient outcomes. All statistical analyses were performed using SPSS software (SPSS software package; SPSS Inc., Chicago, IL) and GraphPad Prism software (GraphPad Software Inc., La Jolla, CA).

3. Results

3.1. Gene expression profiling of HCC

We constructed two SAGE libraries from a HCC–HBV tissue and a corresponding non-cancerous tissue (chronic liver disease (CLD)–HBV). We also used two previously described SAGE libraries, from an HCC–HCV sample and a corresponding non-cancerous tissue sample (CLD–HCV) [4]. After excluding tags detected only once in each library, to avoid the contamination of tags derived from sequence errors, we selected 105,288 tags corresponding to the 9731 genes in all libraries. Using Monte Carlo simulation, we compared the differentially expressed transcripts in HCC and corresponding CLD libraries. Compared with their corresponding CLD libraries, there were statistically significant increases or decreases in 140 transcripts in the HCC–HBV library and in 197 transcripts in the HCC–HCV library ($P < 0.005$).

The HCC–HBV library contained one SAGE tag encoding the HBV–X region, which was increased more than 35-fold compared with its expression in the corresponding CLD–HBV library (Supplemental Table 2). We identified two additional SAGE tags, encoding unknown genes (GTTCTAAAGG, GCATTATGAT), which were expressed more than 10-fold in the HCC–HBV library than in the corresponding CLD–HBV library. The HCC–HBV library also contained tags associated with lipogenesis, at greater than 10-fold abundance, in the HCC–HBV library; these including tags for steroyl-CoA desaturase, fatty acid synthase, and fatty acid desaturase 1.

In contrast, SAGE tags associated with the immune response were up-regulated in the HCC–HCV library. These included tags for Th1-type chemokines, including chemokine ligand 10 (C–X–C motif), chemokine ligand 9 (C–X–C motif), and major histocompatibility complex classes IA and IB (Supplemental Table 3). In addition, tags associated with lipogenesis were increased in the HCC–HCV library, including tags for 3-hydroxy-3-methylglutaryl-coenzyme A synthase 1 and cytochrome P450, family 51, subfamily A, polypeptide 1. Taken together, the differential gene expression patterns may exist in HCC–HBV and HCC–HCV. HBV–X and lipogenesis-related genes are activated in HCC–HBV, whereas genes associated with inflammation as well as lipogenesis are activated in HCC–HCV.

3.2. Analysis of molecular pathways activated in HCC

To further characterize the gene expression patterns of HCC–HBV and HCC–HCV, we performed pathway analysis on SAGE data. Using MetaCore™ software, we found that the candidate transcription factors activated were distinct in each HCC library (Table 1). Several of these transcription factors, including NF-κB, c-Myc, c-Jun, and HNF4-α, have been reported to be activated in HCC [26–29]. In addition, our findings indicated that the transcription factor *SREBF1* may be activated in both HCC–HBV and HCC–HCV (to avoid a confusion, we use HUGO symbol *SREBF1* to indicate both gene/protein name).

Table 1
Candidate transcription factors that regulate molecular pathways activated in HCC.

SAGE library	Transcription factor	Molecular processes	*P*-value
HCC–HCV	NF-κB	Antigen presentation Antigen processing Defense response Immune response	0.004
	SREBF1	Cholesterol biosynthesis Lipid biosynthesis β-Glucoside transport Negative regulation of lipoprotein metabolism	0.05
	SP1	Electron transport; drug metabolism Oxygen and reactive oxygen species metabolism Cell-substrate junction assembly; wound healing	0.05
	IRF1	Immune response Antigen presentation; antigen processing Defense response; positive regulation of cell	0.05
HCC–HBV	HNF4-α	Lipid transport Fatty acid metabolism Smooth muscle cell proliferation	0.002
	HNF1	Acute-phase response; lipid transport Negative regulation of lipid catabolism β-Glucoside transport Negative regulation of lipoprotein metabolism	0.01
	SP1	Zinc ion homeostasis; response to biotic stimulus Nitric oxide mediated signal transduction Copper ion homeostasis; fatty acid biosynthesis	0.01
	c-Jun	Progesterone catabolism; progesterone metabolism Regulation of lipid metabolism; Prostaglandin metabolism	0.03
	C/EBP-α	Lipid transport; negative regulation of lipid catabolism Negative regulation of lipoprotein metabolism β-Glucoside transport Positive regulation of interleukin-8 biosynthesis	0.03
	SREBF1	Lipid biosynthesis; fatty acid biosynthesis Fatty acid metabolism Negative regulation of lipid catabolism Negative regulation of lipoprotein metabolism	0.03
	c-Myc	Fatty acid biosynthesis; fatty acid metabolism Fatty acid desaturation; Activation of pro-apoptotic gene products Release of cytochrome c from mitochondria	0.03
	USF1	Fatty acid metabolism Smooth muscle cell proliferation	0.03
	PPAR-α	Fatty acid metabolism Smooth muscle cell proliferation	0.03
	COUP-TFI	Lipid transport Smooth muscle cell proliferation	0.03
	C/EBP-β	Acute-phase response Regulation of interleukin-6 biosynthesis Fat cell differentiation Inflammatory response	0.03

These findings were evaluated by other pathway analysis software, Ingenuity Pathways Analysis (IPA). We applied the signaling network analysis to the transcripts up-regulated in the HCC libraries ($P < 0.005$). We found that the top signaling network activated in HCC–HBV contained several pathways involved in ERK/MAPK signaling, PPAR signaling, linoleic acid metabolism, and fatty acid metabolism (Supplemental Fig. 2A). Similarly, pathways involved in interferon signaling, NF-κB signaling, antigen presentation, PPAR signaling, linoleic acid metabolism, and fatty acid metabolism were included in the top signaling network activated in HCC–HCV (Supplemental Fig. 2B). Consistent with the results of transcription factor analysis by MetaCore™, pathway analysis indicated that *SREBF1* participates in the lipogenesis pathway in both HCC–HBV and HCC–HCV (blue nodes in Supplemental Fig. 2A and B). *SREBF1*, a major regulator of the lipogenesis pathway, binds to sterol regulatory elements on the genome [30], but less is known about its role in

HCC [31]. We therefore focused on the role of *SREBF1* signaling in HCC.

3.3. Validation of SAGE and signaling network analysis

We performed real-time RT-PCR analysis of *SREBF1* and three representative target genes (*SCD*, *FADS1*, and *FASN*) [20] on 44 samples not used for SAGE. We found that the levels of *SREBF1*, *SCD*, and *FASN* mRNAs were higher in HCC tissues and CLD tissues compared with normal liver, and that these differences were statistically significant (Fig. 1A). We further compared the expression of *SREBF1*, *FADS1*, and *FASN* between HCC and non-cancerous liver tissues, and identified the overexpression of *SREBF1* in HCC with statistical significance (Supplemental Fig. 3). Scatter plot analysis showed that the expression levels of *SREBF1* were correlated with those of *FADS1* ($R = 0.57$, $P < 0.0001$), *SCD* ($R = 0.82$, $P < 0.0001$), and *FASN* ($R = 0.74$, $P < 0.0001$) (Fig. 1B).

Since the mammalian genome encodes two *SREBF1* isoforms, *SREBF1a* and *SREBF1c* [22], we performed semi-quantitative RT-PCR with isoform specific primers to determine which of these isoforms was up-regulated in HCC. We found that *SREBF1c* mRNA, but not *SREBF1a* mRNA, was up-regulated in HCC compared with adjacent non-cancerous liver and normal liver tissues (Supplemental Fig. 4A).

3.4. Functional assay of the lipogenesis pathway in cell lines

Although genome-wide expression profiling showed that the lipogenesis pathway was activated in HCC possibly through up-regulation of *SREBF1*, it was not clear that this pathway played a role in HCC growth. To investigate the role of lipogenesis in HCC cell proliferation, we transfected two short interfering (si)-RNAs (*SREBF1*-1 and *SREBF1*-2) targeting *SREBF1* into the HuH7 and Hep3B cells. These cell lines have no chromosome amplification or deletion on 17p11, on which *SREBF1* is located [32]. Transfection of the si-RNA constructs for *SREBF1*-1 or *SREBF1*-2 decreased expression of *SREBF1* 90% and 70%, respectively, and the expression of both *SCD* and *FADS1* 70% and 60%, respectively (Fig. 2A). Because differences in *SREBF1c* and *SREBF1a* *sequence alignments* are very small, we could not design si-RNAs specifically targeting *SREBF1c*. We therefore checked the effect of si-RNAs on the expression of the *SREBF1* isoforms. We found that the expression of *SREBF1c* was relatively more suppressed than that of *SREBF1a* (Supplemental Fig. 4B), which may have been associated with the higher expression of *SREBF1a* than *SREBF1c* in cultured cell lines [25].

We found that the growth of these transfected cells was significantly inhibited at 72 h compared with mock transfected cells (Fig. 2B and Supplemental Fig.5A). Examination of anchorage independent cell growth showed strong suppression by deactivation of the lipogenesis pathway (Fig. 2C). Because insulin-like growth factor (IGF) is known to induce cancer cell proliferation through activation of PI3-kinase signaling followed by *SREBF1* induction, we investigated the effect of *SREBF1* knockdown on IGF2 mediated cell proliferation. Interestingly, *SREBF1* knockdown abrogated the IGF2 dependent cell proliferation (Supplemental Fig. 5B). Moreover, both the TUNEL assay and annexin V staining showed that transfection of *SREBF1* si-RNAs increased apoptosis compared with mock transfected cells (Fig. 2D and E).

We further investigated the role of *SREBF1* overexpression on cell growth *in vitro*. We transiently transfected control pCMV7 plasmids or pCMV7-*SREBF1c* plasmids (Fig. 3A), and cell proliferation was enhanced in *SREBF1* overexpressing cells compared with the control in both HuH7 and Hep3B cells evaluated by focus assay (Fig. 3B and supplemental Fig. 6). Furthermore, overexpression of *SREBF1* intensified the phosphorylation of GSK-3β, one of the major kinase phosphorylated by the activation of IGF signaling, in a dose-dependent manner (Fig. 3C).

3.5. SREBF1 Expression and prognosis

Since the above results indicated that *SREBF1* signaling may play an important role on tumor cell growth, we investigated the relationship between *SREBF1* expression and mortality in 54 HCC patients by IHC. When we examined the expression of *SREBF1* in HCC tissues and adjacent non-cancerous liver tissues, we identified the increase of the cytoplasmic *SREBF1* staining in a subset of HCC (Fig. 4A). We evaluated the expression of *SREBF1* in HCC and classified 4, 30, and 20 HCCs as *SREBF1*-negative, *SREBF1*-low, and *SREBF1*-high HCC, respectively (Fig. 4B and Supplemental Fig. 1). We could not detect any differences of clinico-pathological characteristics between *SREBF1*-high HCC and *SREBF1*-low/-negative HCC including histological steatosis (Supplemental Table4). Since the seven of these HCC samples were also used for real-time RT-PCR analysis, we investigated the relation of *SREBF1* RNA and protein expression (Fig. 4C). *SREBF1*RNA expression was significantly higher in *SREBF1*-high HCC than in *SREBF1*-low/-negative HCC with statistical significance ($P = 0.03$). Then we examined the cell proliferation of these HCC samples by PCNA staining. Notably, PCNA indexes were significantly higher in *SREBF1*-high HCC than *SREBF1*-low/-negative HCC with statistical significance ($P < 0.001$) (Fig. 4D). We further investigated the relationship between *SREBF1*

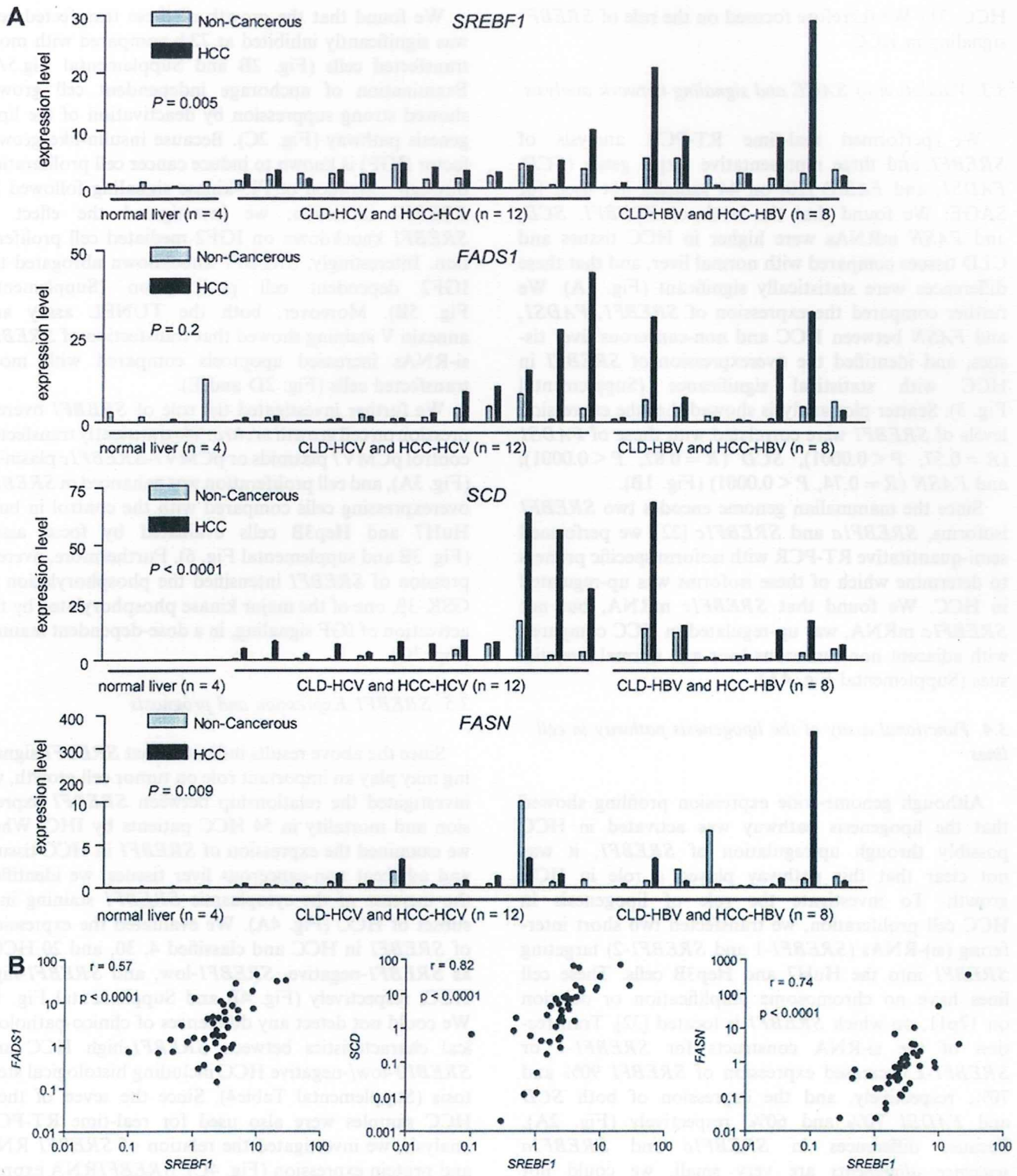

Fig. 1. (A) Real-time quantitative RT-PCR analysis. RNA was isolated from 44 tissue samples: 20 HCC, 20 corresponding CLD, and four normal liver samples. Differential expression of each gene among normal liver tissues, CLD tissues, and HCC tissues was examined by Kruskal–Wallis tests. (B) Scatter plot analysis. Gene expression levels of *FADS1*, *SCD* and *FASN* were well-correlated with those of *SREBF1*, as shown by Spearman's correlation coefficients.

protein expression and prognosis. Kaplan–Meier survival analysis showed a significant relationship between poor survival and high *SREBF1* protein expression ($P = 0.04$; Fig. 4E). Univariate Cox regression analysis showed a correlation between high *SREBF1* protein expression and high risk of mortality with statistical

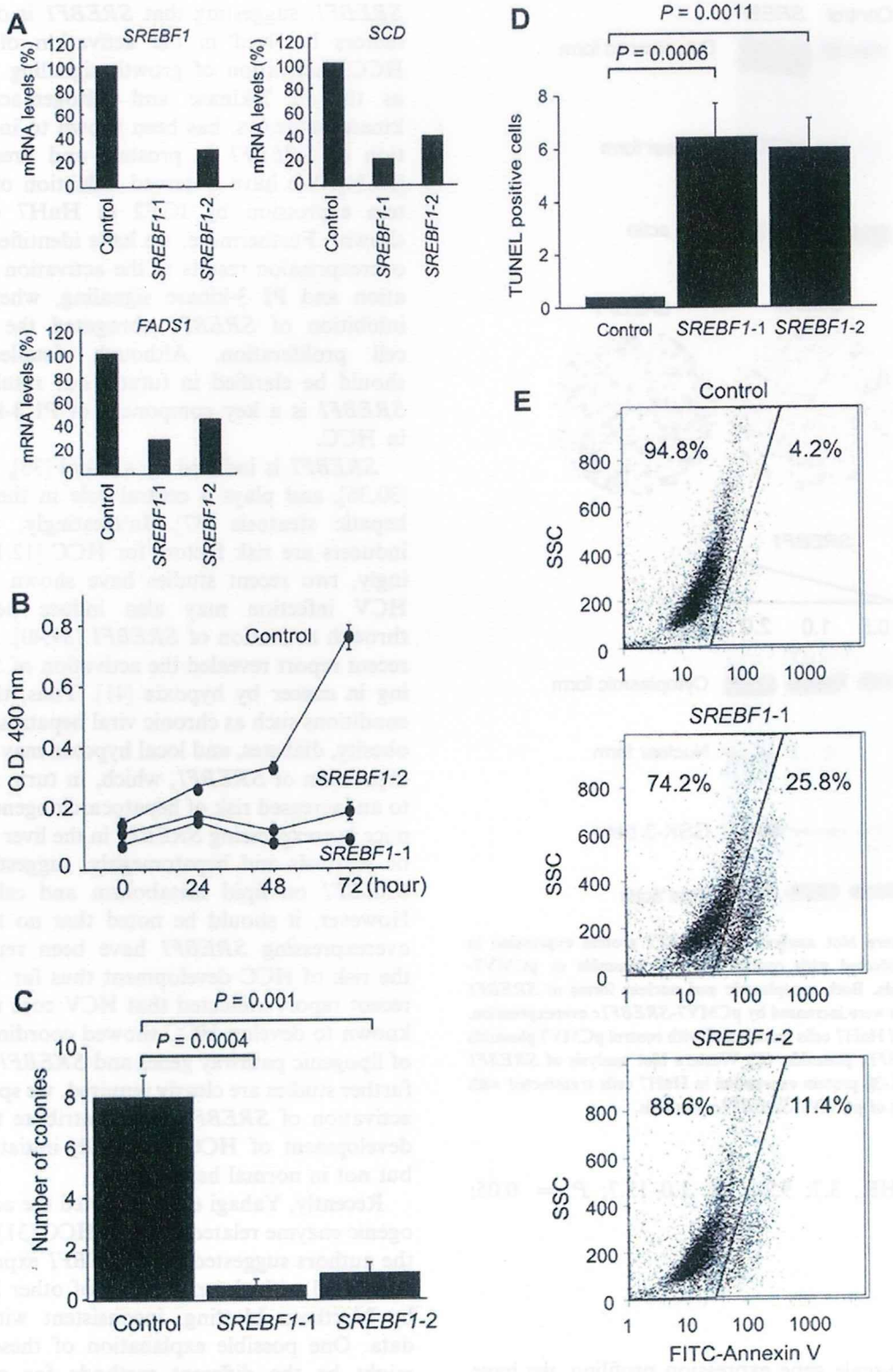

Fig. 2. (A) Effect of RNA interference targeting *SREBF1* in HuH7 cells. Expression levels of *SREBF1* mRNA were reduced by si-RNAs targeting different exons in *SREBF1*. Transcripts of *FADS1* and *SCD* were also down-regulated, showing transcriptional deactivation of the lipogenesis pathway. (B) Cell proliferation assay. Deactivation of the lipogenesis pathway severely reduced cell growth in HuH7 cells. (C) Soft agar assay. Deactivation of the lipogenesis pathway inhibited anchorage independent cell growth in HuH7 cells. (D) TUNEL assay. Deactivation of the lipogenesis pathway significantly increased the number of TUNEL-positive cells in HuH7 cells. (E) Annexin V staining evaluated by flow cytometer. Deactivation of the lipogenesis pathway significantly increased the number of annexin V positive cells in HuH7 cells.

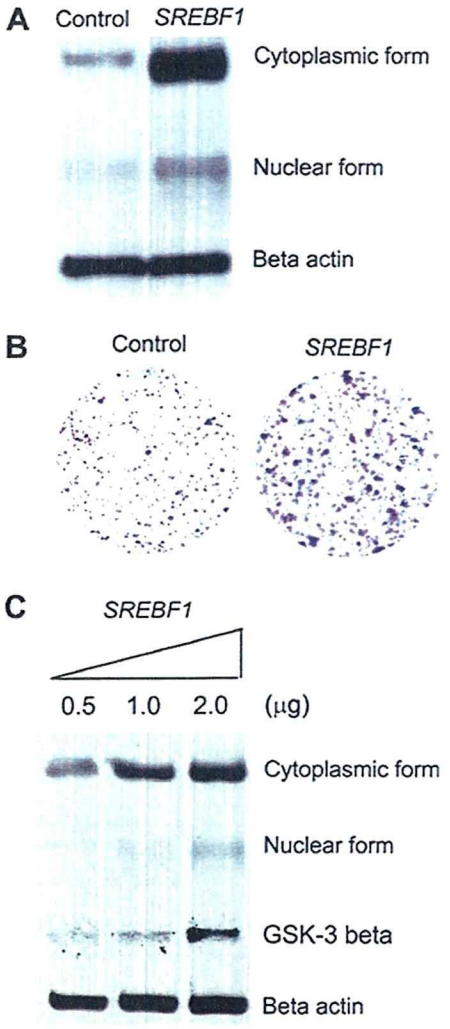

Fig. 3. (A) Western blot analysis of *SREBF1* protein expression in HuH7 cells transfected with control pCMV7 plasmids or pCMV7-*SREBF1c* plasmids. Both cytoplasmic and nuclear forms of *SREBF1* protein expression were increased by pCMV7-*SREBF1c* overexpression. (B) Focus assay of HuH7 cells transfected with control pCMV7 plasmids or pCMV7-*SREBF1c* plasmids. (C) Western blot analysis of *SREBF1* and phospho-GSK-3β protein expression in HuH7 cells transfected with indicated amounts of pCMV7-*SREBF1c* plasmids.

significance (HR, 3.7; 95% CI, 1.0–13.7; $P = 0.05$; Table 2).

4. Discussion

Using large-scale gene expression profiling, we have shown that the lipogenesis pathway is transcriptionally activated in HCC. Our SAGE profiles will be available on our homepage (http://www.intmedkanazawa.jp/) and will be submitted to the Gene Expression Omnibus (http://www.ncbi.nlm.nih.gov/geo/).

We found that the levels of expression of *FADS1*, *SCD*, and *FASN* were each correlated with those of *SREBF1*, suggesting that *SREBF1* is one of the main factors involved in the activation of lipogenesis in HCC. Activation of growth signaling pathways, such as the PI 3-kinase and mitogen-activated protein kinase pathways, has been shown to induce up-regulation of *SREBF1* in prostate and breast cancer cells [33,34]. We have observed induction of *SREBF1* protein expression by IGF2 in HuH7 cells (data not shown). Furthermore, we have identified that *SREBF1* overexpression results in the activation of cell proliferation and PI 3-kinase signaling, whereas expression inhibition of *SREBF1* abrogated the IGF2 induced cell proliferation. Although detailed mechanisms should be clarified in future, our results suggest that *SREBF1* is a key component of PI 3-kinase signaling in HCC.

SREBF1 is induced by alcohol [35], insulin, and fat [30,36], and plays a central role in the mechanism of hepatic steatosis [37]. Interestingly, these *SREBF1* inducers are risk factors for HCC [12,13,38,14]. Strikingly, two recent studies have shown that HBV and HCV infection may also induce hepatic steatosis through activation of *SREBF1* [39,40]. Furthermore, a recent report revealed the activation of *SREBF1* signaling in cancer by hypoxia [41]. Thus, these pathologic conditions such as chronic viral hepatitis, alcohol abuse, obesity, diabetes, and local hypoxia may up-regulate the expression of *SREBF1*, which, in turn, may contribute to an increased risk of hepatocarcinogenesis. Transgenic mice overexpressing *SREBF1* in the liver exhibited hepatic steatosis and hepatomegaly, suggesting the role of *SREBF1* on lipid metabolism and cell proliferation. However, it should be noted that no transgenic mice overexpressing *SREBF1* have been reported to have the risk of HCC development thus far. Interestingly, a recent report indicated that HCV core transgenic mice known to develop HCC showed coordinated activation of lipogenic pathway genes and *SREBF1* [42]. Although further studies are clearly required, we speculate that the activation of *SREBF1* may contribute to promote the development of HCC in already-initiated hepatocytes but not in normal hepatocytes.

Recently, Yahagi et al. reported the activation of lipogenic enzyme related genes in HCC [31]. In that paper, the authors suggested that *SREBF1* expression was not correlated with the expression of other lipogenic genes by Northern blotting, inconsistent with our current data. One possible explanation of these discrepancies might be the different methods for quantitation of mRNA, and we believe that real-time RT-PCR method used in our study would be more accurate. In addition, we evaluated the expression of *SREBF1* and lipogenic genes using more samples (a total of 44 liver and HCC tissues) than Yahagi et al did (10 HCC tissues). Furthermore, a recent paper indicated the coordinated activation of *SREBF1* and lipogenic genes in HCC

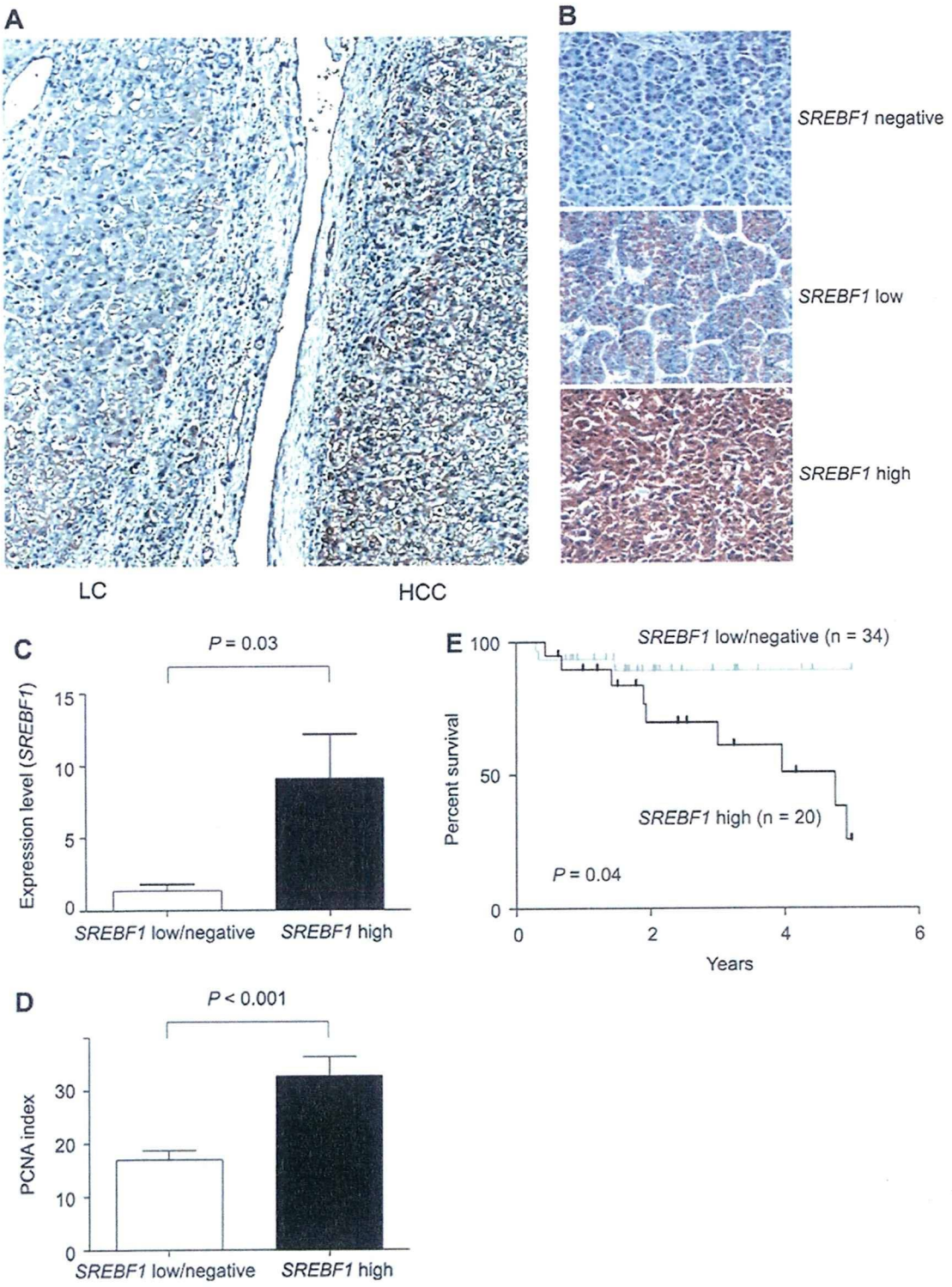

Fig. 4. (A) A photomicrograph of an HCC with adjacent non-cancerous cirrhotic liver stained with anti-*SREBF1* antibodies. (B) Representative photomicrographs of *SREBF1*-negative-, *SREBF1*-low-, and *SREBF1*-high-HCC tissues stained with anti- *SREBF1* antibodies. (C) *SREBF1* gene expression by real-time RT-PCR according to protein expression status assessed by IHC. *SREBF1* was highly expressed in *SREBF1*-high HCC ($P = 0.03$). (D) SREBF1 expression and cell proliferation in HCC. PCNA indexes in *SREBF1*-high HCC were higher than those in *SREBF1*-low/-negative HCC with statistical significance ($P < 0.001$). (E) Kaplan–Meier plots of 54 HCC patients analyzed by immunohistochemistry. The differences between *SREBF1*-high and -low/-negative HCC were analyzed by log-rank test.

developed in the liver of HCV core transgenic mice [42], strongly support our data. Although further studies using large numbers of HCC tissues may be required, these data suggest that the lipogenic gene activation seems to be mediated, at least in part, by *SREBF1* expression in HCC.

Table 2
Univariate Cox regression analysis of survival relative to *SREBF1* protein expression and clinicopathological parameters.

Variables (*n*)	HR (95% CI)	*P*-value
SREBF1 and mortality ($n = 54$)		
Tumor size		
<3 cm ($n = 37$)	1	
⩾3 cm ($n = 17$)	2.2 (0.6–8.3)	0.2
pTNM stage		
I, II ($n = 45$)	1	
III, IV ($n = 9$)	2.0 (0.4–9.4)	0.4
Serum AFP		
<20 ng/ml ($n = 35$)	1	
⩾20 ng/ml (n = 19)	1.5 (0.4–5.4)	0.5
SREBF1		
Low ($n = 34$)	1	
High ($n = 20$)	3.7 (1.0–13.7)	0.05

Because the majority of our HCC patients analyzed had Child–Pugh class A scores and about 70% had tumors less than 3 cm in diameter, all were expected to have a good prognosis. Indeed, patient survival in this cohort was not segregated by tumor size or pTNM stage (Table 2). Although the sample size was relatively small, we found that enhanced expression of *SREBF1* was a prognostic factor for mortality in HCC possibly due to the highly proliferative nature. Activation of lipogenesis pathways, as shown by overexpression of *FASN*, has been found to correlate with high mortality in breast, prostate, and lung cancer [43], suggesting that activation of lipogenesis may be a fundamental characteristic of cancer with poor prognosis. Thus, *SREBF1* expression may be a good biomarker for HCC classification, a finding that should be validated in a large scale cohort. Because deactivation of the lipogenesis pathway by inhibition of *SREBF1* gene expression could inhibit HCC cell growth *in vitro*, *SREBF1* may be a good target for pharmaceutical intervention in these tumors.

In conclusion, our genome-wide gene expression profiling analyses found that the lipogenesis pathway was activated in a subset of HCC. *SREBF1*, which activates the lipogenesis pathway, may be a good biomarker for HCC prognosis and may be a good target for therapeutic intervention.

Acknowledgements

We are grateful to the members of The Liver Disease Center at Kanazawa University Hospital for providing data of human liver tissue samples. We would also like to thank Dr. Hitoshi Shimano for providing invaluable reagents.

Appendix A. Supplementary data

Supplementary data associated with this article can be found, in the online version, at doi:10.1016/j.jhep.2008.07.036.

References

[1] El-Serag HB, Mason AC. Rising incidence of hepatocellular carcinoma in the United States. N Engl J Med 1999;340:745–750.
[2] Bosch FX, Ribes J, Diaz M, Cleries R. Primary liver cancer: worldwide incidence and trends. Gastroenterology 2004;127:S5–S16.
[3] Wang XW, Hussain SP, Huo TI, Wu CG, Forgues M, Hofseth LJ, et al. Molecular pathogenesis of human hepatocellular carcinoma. Toxicology 2002;181-182:43–47.
[4] Yamashita T, Kaneko S, Hashimoto S, Sato T, Nagai S, Toyoda N, et al. Serial analysis of gene expression in chronic hepatitis C and hepatocellular carcinoma. Biochem Biophys Res Commun 2001;282:647–654.
[5] Shirota Y, Kaneko S, Honda M, Kawai HF, Kobayashi K. Identification of differentially expressed genes in hepatocellular carcinoma with cDNA microarrays. Hepatology 2001;33:832–840.
[6] Okabe H, Satoh S, Kato T, Kitahara O, Yanagawa R, Yamaoka Y, et al. Genome-wide analysis of gene expression in human hepatocellular carcinomas using cDNA microarray: identification of genes involved in viral carcinogenesis and tumor progression. Cancer Res 2001;61:2129–2137.
[7] Xu XR, Huang J, Xu ZG, Qian BZ, Zhu ZD, Yan Q, et al. Insight into hepatocellular carcinogenesis at transcriptome level by comparing gene expression profiles of hepatocellular carcinoma with those of corresponding noncancerous liver. Proc Natl Acad Sci USA 2001;98:15089–15094.
[8] Iizuka N, Oka M, Yamada-Okabe H, Mori N, Tamesa T, Okada T, et al. Comparison of gene expression profiles between hepatitis B virus- and hepatitis C virus-infected hepatocellular carcinoma by oligonucleotide microarray data on the basis of a supervised learning method. Cancer Res 2002;62:3939–3944.
[9] Thorgeirsson SS, Grisham JW. Molecular pathogenesis of human hepatocellular carcinoma. Nat Genet 2002;31:339–346.
[10] Lee JS, Thorgeirsson SS. Genome-scale profiling of gene expression in hepatocellular carcinoma: classification, survival prediction, and identification of therapeutic targets. Gastroenterology 2004;127:S51–S55.
[11] Suriawinata A, Xu R. An update on the molecular genetics of hepatocellular carcinoma. Semin Liver Dis 2004;24:77–88.
[12] El-Serag HB, Tran T, Everhart JE. Diabetes increases the risk of chronic liver disease and hepatocellular carcinoma. Gastroenterology 2004;126:460–468.
[13] Hassan MM, Hwang LY, Hatten CJ, Swaim M, Li D, Abbruzzese JL, et al. Risk factors for hepatocellular carcinoma: synergism of alcohol with viral hepatitis and diabetes mellitus. Hepatology 2002;36:1206–1213.
[14] Ohata K, Hamasaki K, Toriyama K, Matsumoto K, Saeki A, Yanagi K, et al. Hepatic steatosis is a risk factor for hepatocellular carcinoma in patients with chronic hepatitis C virus infection. Cancer 2003;97:3036–3043.
[15] Calle EE, Rodriguez C, Walker-Thurmond K, Thun MJ. Overweight, obesity, and mortality from cancer in a prospectively studied cohort of US adults. N Engl J Med 2003;348:1625–1638.
[16] Walsh MJ, Vanags DM, Clouston AD, Richardson MM, Purdie DM, Jonsson JR, et al. Steatosis and liver cell apoptosis in chronic hepatitis C: a mechanism for increased liver injury. Hepatology 2004;39:1230–1238.

[17] Powell EE, Jonsson JR, Clouston AD. Steatosis: co-factor in other liver diseases. Hepatology 2005;42:5–13.
[18] Velculescu VE, Zhang L, Vogelstein B, Kinzler KW. Serial analysis of gene expression. Science 1995;270:484–487.
[19] Yamashita T, Hashimoto S, Kaneko S, Nagai S, Toyoda N, Suzuki T, et al. Comprehensive gene expression profile of a normal human liver. Biochem Biophys Res Commun 2000;269:110–116.
[20] Desmet VJ, Gerber M, Hoofnagle JH, Manns M, Scheuer PJ. Classification of chronic hepatitis: diagnosis, grading and staging. Hepatology 1994;19:1513–1520.
[21] Polyak K, Xia Y, Zweier JL, Kinzler KW, Vogelstein B. A model for p53-induced apoptosis. Nature 1997;389:300–305.
[22] Yokoyama C, Wang X, Briggs MR, Admon A, Wu J, Hua X, et al. SREBP-1, a basic-helix–loop-helix–leucine zipper protein that controls transcription of the low density lipoprotein receptor gene. Cell 1993;75:187–197.
[23] Wang HC, Chang WT, Chang WW, Wu HC, Huang W, Lei HY, et al. Hepatitis B virus pre-S2 mutant upregulates cyclin A expression and induces nodular proliferation of hepatocytes. Hepatology 2005;41:761–770.
[24] Takeba Y, Kumai T, Matsumoto N, Nakaya S, Tsuzuki Y, Yanagida Y, et al. Irinotecan activates p53 with its active metabolite, resulting in human hepatocellular carcinoma apoptosis. J Pharmacol Sci 2007;104:232–242.
[25] Closset J, Van de Stadt J, Delhaye M, El Nakadi I, Lambilliotte JP, Gelin M. Hepatocellular carcinoma: surgical treatment and prognostic variables in 56 patients. Hepatogastroenterology 1999;46:2914–2918.
[26] Arsura M, Cavin LG, Calvisi DF, Thorgeirsson SS, Eferl R, Ricci R, et al. Nuclear factor-kappaB and liver carcinogenesis. Cancer Lett 2005;229:157–169.
[27] Calvisi DF, Thorgeirsson SS. Molecular mechanisms of hepatocarcinogenesis in transgenic mouse models of liver cancer. Toxicol Pathol 2005;33:181–184.
[28] Eferl R, Ricci R, Kenner L, Zenz R, David JP, Rath M, et al. Liver tumor development. c-Jun antagonizes the proapoptotic activity of p53. Cell 2003;112:181–192.
[29] Xu L, Hui L, Wang S, Gong J, Jin Y, Wang Y, et al. Expression profiling suggested a regulatory role of liver-enriched transcription factors in human hepatocellular carcinoma. Cancer Res 2001;61:3176–3181.
[30] Horton JD, Goldstein JL, Brown MS. SREBPs: activators of the complete program of cholesterol and fatty acid synthesis in the liver. J Clin Invest 2002;109:1125–1131.
[31] Yahagi N, Shimano H, Hasegawa K, Ohashi K, Matsuzaka T, Najima Y, et al. Co-ordinate activation of lipogenic enzymes in hepatocellular carcinoma. Eur J Cancer 2005;41:1316–1322.
[32] Kawaguchi K, Honda M, Yamashita T, Shirota Y, Kaneko S. Differential gene alteration among hepatoma cell lines demonstrated by cDNA microarray-based comparative genomic hybridization. Biochem Biophys Res Commun 2005;329:370–380.
[33] Van de Sande T, De Schrijver E, Heyns W, Verhoeven G, Swinnen JV. Role of the phosphatidylinositol 3′-kinase/PTEN/Akt kinase pathway in the overexpression of fatty acid synthase in LNCaP prostate cancer cells. Cancer Res 2002;62:642–646.
[34] Yang YA, Han WF, Morin PJ, Chrest FJ, Pizer ES. Activation of fatty acid synthesis during neoplastic transformation: role of mitogen-activated protein kinase and phosphatidylinositol 3-kinase. Exp Cell Res 2002;279:80–90.
[35] You M, Fischer M, Deeg MA, Crabb DW. Ethanol induces fatty acid synthesis pathways by activation of sterol regulatory element-binding protein (SREBP). J Biol Chem 2002;277:29342–29347.
[36] Muller-Wieland D, Kotzka J. SREBP-1: gene regulatory key to syndrome X? Ann NY Acad Sci 2002;967:19–27.
[37] Sekiya M, Yahagi N, Matsuzaka T, Najima Y, Nakakuki M, Nagai R, et al. Polyunsaturated fatty acids ameliorate hepatic steatosis in obese mice by SREBP-1 suppression. Hepatology 2003;38:1529–1539.
[38] Marrero JA, Fontana RJ, Su GL, Conjeevaram HS, Emick DM, Lok AS. NAFLD may be a common underlying liver disease in patients with hepatocellular carcinoma in the United States. Hepatology 2002;36:1349–1354.
[39] Kim KH, Shin HJ, Kim K, Choi HM, Rhee SH, Moon HB, et al. Hepatitis B virus X protein induces hepatic steatosis via transcriptional activation of SREBP1 and PPARgamma. Gastroenterology 2007;132:1955–1967.
[40] Waris G, Felmlee DJ, Negro F, Siddiqui A. Hepatitis C virus induces proteolytic cleavage of sterol regulatory element binding proteins and stimulates their phosphorylation via oxidative stress. J Virol 2007;81:8122–8130.
[41] Furuta E, Pai SK, Zhan R, Bandyopadhyay S, Watabe M, Mo YY, et al. Fatty acid synthase gene is up-regulated by hypoxia via activation of Akt and sterol regulatory element binding protein-1. Cancer Res 2008;68:1003–1011.
[42] Tanaka N, Moriya K, Kiyosawa K, Koike K, Gonzalez FJ, Aoyama T. PPARalpha activation is essential for HCV core protein-induced hepatic steatosis and hepatocellular carcinoma in mice. J Clin Invest 2008;118:683–694.
[43] Kuhajda FP. Fatty acid synthase and cancer: new application of an old pathway. Cancer Res 2006;66:5977–5980.

Strain-Dependent Viral Dynamics and Virus-Cell Interactions in a Novel *In Vitro* System Supporting the Life Cycle of Blood-Borne Hepatitis C Virus

Hussein Hassan Aly,[1,2] Yue Qi,[3] Kimie Atsuzawa,[4] Nobuteru Usuda,[4] Yasutsugu Takada,[5] Masashi Mizokami,[6] Kunitada Shimotohno,[7] and Makoto Hijikata[1,3]

We developed an *in vitro* system that can be used for the study of the life cycle of a wide variety of blood-borne hepatitis C viruses (HCV) from various patients using a three-dimensional hollow fiber culture system and an immortalized primary human hepatocyte (HuS-E/2) cell line. Unlike the conventional two-dimensional culture, this system not only enhanced the infectivity of blood-borne HCV but also supported its long-term proliferation and the production of infectious virus particles. Both sucrose gradient fractionation and electron microscopy examination showed that the produced virus-like particles are within a similar fraction and size range to those previously reported. Infection with different HCV strains showed strain-dependent different patterns of HCV proliferation and particle production. Fluctuation of virus proliferation and particle production was found during prolonged culture and was found to be associated with change in the major replicating virus strain. Induction of cellular apoptosis was only found when strains of HCV-2a genotype were used for infection. Interferon-alpha stimulation also varied among different strains of HCV-1b genotypes tested in this study. *Conclusion:* These results suggest that this *in vitro* infection system can reproduce strain-dependent events reflecting viral dynamics and virus-cell interactions at the early phase of blood-borne HCV infection, and that this system can allow the development of new anti-HCV strategies specific to various HCV strains. (HEPATOLOGY 2009;50:689-696.)

Hepatitis C virus (HCV) is a serious problem worldwide, with 3% of the world's population chronically infected.[1] Chronic infection with HCV may lead to high rates of liver cirrhosis and hepatocellular carcinoma.[2] Because the HCV standard therapy is still insufficient for treating many patients,[3] the development of more effective and less toxic anti-HCV agents is desired. The virological studies required to reach this goal need reproducible and efficient HCV proliferation in cell culture. An *in vitro* infection system using recombinant HCV-JFH1 was developed. In this system, HuH7 cells transfected with *in vitro*-synthesized JFH1-RNA were

Abbreviations: 2D, two-dimensional; 2D-HuS-E/2, HuS-E/2 cells cultured in two-dimensional condition; 3D, three-dimensional; 3D/HF, 3D hollow fibers; 3D-HuS-E/2, HuS-E/2 cells cultured in three-dimensional condition in the hollow fibers; HCV, hepatitis C virus; IFN-α, interferon alpha; LDH, lactate dehydrogenase; p.i., postinfection; RFB, radial-flow bioreactor; RT-PCR, reverse transcription polymerase chain reaction.

From the [1]Laboratory of Human Tumor Viruses, Institute for Virus Research, Kyoto University, Kyoto, Japan; [2]Hepatology Department, National Hepatology and Tropical Medicine Research Institute, Cairo, Egypt; [3]Laboratory of Viral Oncology, Graduate School of Biostudies, Kyoto University, Kyoto, Japan; [4]Department of Anatomy, Fujita Health University School of Medicine, Toyoake, Japan; [5]Department of Surgery, Division of Hepato-Pancreato-Biliary and Transplant Surgery, Graduate School of Medicine, Kyoto University, Kyoto, Japan; [6]Research Center for Hepatitis and Immunology, International Medical Center of Japan Kounodai Hospital, Ichikawa, Japan; [7]Center for Human Metabolomic Systems Biology, Keio University, Tokyo, Japan.

Received November 12, 2008; accepted April 9, 2009.

Supported by grants-in-aid from the Ministry of Health, Labor and Welfare of Japan; by grants-in-aid from Japan Health Sciences Foundation; and by grants-in-aid for scientific research from Ministry of Education, Sports, Culture, and Technology of Japan.

Address reprint requests to: Kunitada Shimotohno, Ph.D., Center for Human Metabolomic Systems Biology, Keio University, 35, Shinano-machi, Shinjuku-ku, Tokyo, 160-8582, Japan. E-mail: shimkuni@z8.keio.jp; fax: 81-3-5363-3592; or Makoto Hijikata, Ph.D., Laboratory of Human Tumor Viruses, Institute for Virus Research, Kyoto University, 53, Kawaharacho, Shogoin, Sakyoku, Kyoto, 606-8507, Japan. E-mail: mhijikat@virus.kyoto-u.ac.jp; fax: 81-75-751-3998.

Copyright © 2009 by the American Association for the Study of Liver Diseases.

Published online in Wiley InterScience (www.interscience.wiley.com).

DOI 10.1002/hep.23034

Potential conflict of interest: Nothing to report.

Additional Supporting Information may be found in the online version of this article.

shown to secrete infectious viral particles.[4] This system, however, requires the combination of HuH-7-derived cell lines and JFH1-based constructs, limiting its usefulness for studying other HCV strains. Because HuH-7 cells cannot support the complete life cycle of blood-borne HCV (bbHCV) derived from clinical samples,[5] this system is insufficient for studying all the events related to bbHCV infection.

Many researchers have attempted to develop an *in vitro* system for bbHCV.[6-8] These current systems, however, are still insufficient due to their low efficiency for infectivity and replication of bbHCV. Working toward this same goal, we recently established immortalized primary human hepatocyte cell lines by transducing them with E6 and E7 genes from the human papilloma virus 18.[5,9] As expected, we observed improved infection and replication of bbHCV especially in one of these cell lines (HuS-E/2 cells) that showed a similar expression profile to that of human primary hepatocytes, but this strategy did not improve production of infectious particles.

Recently, a hybrid artificial liver support system was developed using animal hepatocytes cultured in a three-dimensional hollow fiber (3D/HF) system. This bioartificial liver showed several characteristic features of liver tissue for more than 4 months.[10-12] By growing our HuS-E/2 cells in a similar 3D culture[5] the gene expression profile was improved to more closely match that of human primary hepatocytes. Because the 3D cell culture condition more closely reproduces the *in vivo* environment of hepatocytes,[13] culturing these cells in this manner may support the entire HCV life cycle.

In this study we utilized this small 3D culture system and showed it to be ideal for culturing HuS-E/2 cells for the study of bbHCV infection. Using this system we are now able to study the variable patterns of the life cycle of different bbHCV strains as well as HCV-related cellular events.

Materials and Methods

Cell Culture. HuS-E/2 cells were cultured as previously described.[5] For the 3D/HF system, HuS-E/2 suspension was injected into the lumen of HF (Toyobo, Osaka, Japan) made from cellulose acetate and containing pores for nutrients and waste exchange (Supporting Fig. 1). The bundles were centrifuged to induce organoid formation. The cells in the fibers were cultured in 12-well plates (two capillary bundles per well) with gentle rotation using serum-free medium (Toyobo) in a CO_2 incubator at 37°C. The number of cells was adjusted to 3 × 105 cells per two-capillary bundle at the start of each experiment.

RNA Experiments. Total RNA was extracted from two-dimensional (2D) cultured cells, patient sera, or from 100 times concentrated culture medium as previously described.[4,5] For cells cultured in the 3D/HF, sterile scissors were used to cut each fiber into small pieces (1 mm^2 each), which were then solubilized in Sepasol RNA-1 (Nacalai Tesque, Kyoto, Japan). RNA was then extracted according to the manufacturer's protocol. Real-time reverse transcription polymerase chain reaction (RT-PCR) was performed as described.[5]

HCV Infection. HCV infection experiments were carried out using sera from HCV patients. The amount of each inoculum was adjusted so as to add similar amount of HCV-RNA to the medium of the cells. After 24 hours, the cells were washed three times with phosphate-buffered saline (PBS) and cultured for the designated times. To assess the passage of infectivity, 12 mL of culture medium from the primary infected cells was collected, concentrated 100 times by filtration through Amicon Ultra-15, Ultracel-10K filters (Millipore, Carrigtwohill, Cork, Ireland), and 40 μL concentrated medium/well was used to infect naïve HuS-E/2 cells. All experiments were done with approval of the Ethical Committee of Kyoto University. Informed consent from patients was required for this approval.

Cloning and Sequencing. To amplify the complementary DNA (cDNA) fragment corresponding to hypervariable region 1 (HVR-1),[14] a nested RT-PCR was performed using Superscript III (Invitrogen, Carlsbad, CA) and PrimeSTAR HS DNA Polymerase (Takara, Tokyo, Japan). Reaction conditions were adjusted according to the manufacturer's protocol. Primers used were previously described[15] and are shown in Supporting Table 1. PCR products were then purified and cloned using the Zero Blunt TOPO PCR Cloning Kit (Invitrogen). Ten recombinant clones were randomly isolated for each PCR product and sequenced as described.[16]

Quantitative Detection of HCV Core and Interferon alpha (IFN-α) Protein by Enzyme-Linked Immunosorbent Assay (ELISA). The culture medium of infected cells was collected and concentrated 100 times as previously mentioned for the detection of HCV-core, or used directly for detection of IFN-α. HCV core protein was quantified using the Trak-C Core ELISA (Ortho Clinical Diagnostics, Neckargemünd, Germany). IFN-α was quantified using the Human IFN-A ELISA kit (PBL Biomedical Laboratories, Piscataway, NJ). Light absorbance was then measured using a Wallac 1420 multilabel counter (PerkinElmer Life Science, Waltham, MA).

Cytotoxicity Assay. Culture medium was collected from HCV-infected cells and used for measuring lactate dehydrogenase (LDH) levels using an LDH cytotoxicity

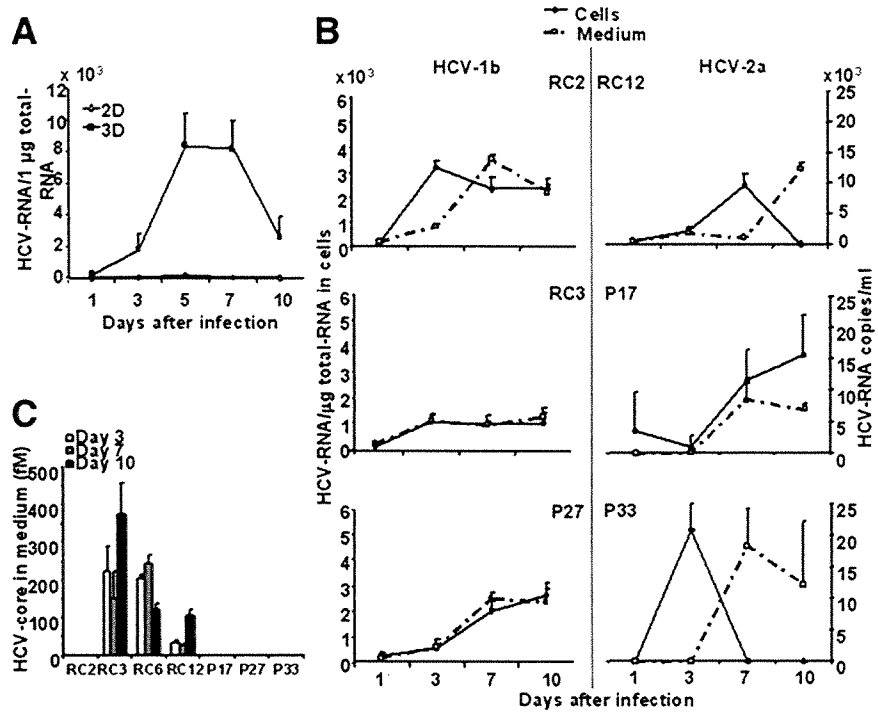

Fig. 1. Infection and proliferation of bbHCV in 3D-HuS-E/2 cells. (A) The quantity of HCV genomic RNA in 1 μg total RNA of 2D- or 3D-HuS-E/2 cells infected with HCV-RC6 was determined at each timepoint after infection by real-time RT-PCR analysis. (B) 3D-HuS-E/2 cells were infected with HCV-1b-containing sera: RC2, RC3, and P27; or HCV-2a-containing sera: 4: RC12, P17, P33. The quantity of HCV genomic RNA in the infected cells was determined as in (A). The culture medium from the last 2 days at each timepoint was collected, concentrated, and the amount of HCV-RNA (B) or HCV-core (C) was measured. Data represent the mean ± standard deviation (SD) of three independent experiments.

detection kit (Takara Biomedicals). Light absorbance was then measured as described above.

Sucrose Density Gradient. The culture medium of the infected cells was collected, concentrated 500 times, and loaded onto a 20%-50% (wt/vol) sucrose gradient containing 50 mM PBS, 100 mM NaCl, and 1 mM EDTA, followed by centrifugation at 100,000*g* for 16 hours at 4°C in a SW41Ti rotor (Beckman, Fullerton, CA). The gradient was fractionated into 31 fractions that were used for HCV-RNA and core detection and HCV infection into naïve cells as described above.

Electron Microscopy. The 1.12 g/mL fraction obtained by the sucrose density gradient showed the secondary infection activity as analyzed by transmission electron microscopy. The fraction was ultracentrifuged and the almost all supernatant was removed. The residual 10 μL of the solution was directly applied to a formvar-carbon grid for negative staining with 1% uranyl acetate solution and observed with an electron microscope (JEOL1010, JEOL, Tokyo, Japan).

Results

HuS-E/2 Cells Cultured in 3D/HF System Are Highly Permissive for Infection and Proliferation of bbHCV. We compared the ability of HuS-E/2 cells cultured in the 3D/HF system (3D-HuS-E/2 cells) to those cultured as a monolayer (2D-HuS/E2 cells) to reproduce infection by HCV genotype 1b (HCV-RC6), derived from patient serum (RC6). The HCV-RC6 RNA levels in the 3D-HuS/E2 cells were significantly higher at all timepoints (Fig. 1A), showing that the 3D/HF system greatly improves the proliferation of bbHCV in HuS-E/2 cells. We observed that both the early stages of infection and the continuous replication of HCV-RC6 in HuS-E/2 cells was improved by 3D/HF culture when the culture conditions were changed after the infection from 3D/HF to 2D and vice versa (Supporting Fig. 2).

As reported,[17] blocking CD81, an HCV-supposed entry receptor, during infection significantly impaired HCV proliferation into 3D-HuS-E/2 cells (Supporting Fig. 3), suggesting that CD81 is essential for HCV infectivity in 3D-HuS-E/2 cells. Although the expression level of CD81 mRNA in 3D-HuS-E/2 cells was observed, no significant change from 2D-HuS/E2 cells was found (data not shown), indicating that the quantity of CD81, at least, is not responsible for the improvement.

We then examined whether this system can be used for proliferation of six different bbHCV samples, three of which are HCV-1b (HCV-RC2, HCV-RC3, and HCV-P27) and three HCV-2a genotypes (HCV-RC12, HCV-P17, and HCV-P33) (Fig. 1B). Proliferation of HCV-RNA in the cells was seen in all six cases, suggesting that this system can be widely used for analysis of infection and proliferation of bbHCV strains. HCV-RNA and HCV-core were also detected in the culture medium (Fig. 1B). Different HCV strains showed variable patterns of proliferation and HCV-core secretion into the medium. Although HCV-core was detected from day 3 onward when